Brief Review

Modern Physics Letters B, Vol. 21, No. 27 (2007) 1807–1830

World Scientific
www.worldscientific.com

ELECTRON EMISSION FROM CARBON NANOTUBES

PARHAM YAGHOOBI and ALIREZA NOJEH*

Department of Electrical and Computer Engineering,
University of British Columbia,
Vancouver, BC V6T 1Z4, Canada
**anojeh@ece.ubc.ca*

Received 29 August 2007

Carbon nanotubes, nanometer-diameter tubes made of carbon atoms, have garnered significant attention from researchers over the past 15 years due to their outstanding properties such as excellent electronic transport characteristics and mechanical strength. Because of their ability to carry extremely high current densities, their high aspect ratio, and small tip radius that enhances an external electric field greatly, one particularly promising area of interest has been the usage of nanotubes as electron sources. In this article we will try to provide an overview of the subject from various experimental and theoretical angles.

Keywords: Carbon nanotubes; field-emission; Fowler–Nordheim model; thermionic emission.

1. Introduction

Electron beams play a very important role in many areas of science and technology, ranging from applications in everyday life such as cathode ray tubes in traditional television sets, to usage in well-established research instruments such as electron microscopes, to cutting-edge research in sophisticated scientific experiments in synchrotrons. Since the associated wavelength of an electron is very small (even sub-angstrom) for electrons with kinetic energies of several kilo electron volts (keV) that are easily achievable in laboratory settings, they can be much more easily focused compared to light beams for applications where a high spatial resolution is needed such as micro- and nano-probing and pattern writing. Significant progress has been made over the last several decades in electron-beam research, both in terms of electron emission from source, as well as beam optics. Current state-of-the-art electron microscopes can easily achieve an imaging resolution of a few nanometers and are routinely used in research (Fig. 1). However, much work still remains to be done in this area. In particular, in many current electron-beam applications, the performance bottleneck is the electron source, i.e. the tip that emits the electrons into vacuum, where they subsequently undergo deflection, focusing, etc. based on the

*Corresponding author.

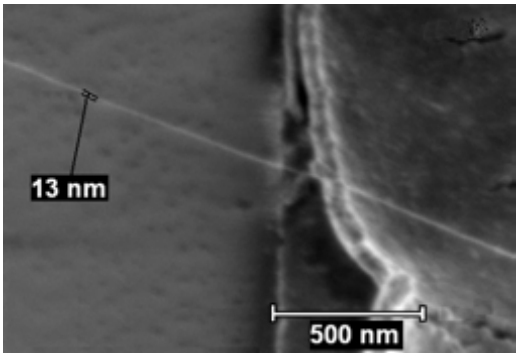

Fig. 1. A high-resolution image of a carbon nanotube suspended over the edge of a peeled metal electrode, obtained in an FEI Sirion scanning electron microscope.

application. For the source, some of the major considerations include being able to generate a high enough current from a very small spot with little noise and fluctuation over extended periods of time. Also, it is important that the generated electrons be very similar (in terms of their energy), in order for the electron-optical system to direct all of them in a similar fashion.

Thus, the field of electron emission is a very active area of research and many scientists and engineers around the world are on the quest for new, improved electron sources. (We use the terms source and emitter interchangeably in this article.) Due to their outstanding electronic and mechanical properties, carbon nanotubes, allotropes of carbon with nanoscale diameters, have attracted much attention during the last decade and a half. One of the main applications they are being researched for is electron emission. In this article, after a brief review of electron emission and introduction of carbon nanotubes, we will provide an overview of the field of electron emission from nanotubes, trying to give the reader a taste of the various aspects of experimental and theoretical work being pursued in this field. Obviously, however, due to the vast literature available, it is not possible in this brief review to cover all the valuable works that have been done on the subject.

2. Electron Emission Mechanisms

There are various well-established mechanisms through which electrons can leave a source and emit into vacuum. In thermionic emission, the source — typically a metal with a high melting point such as tungsten — is heated to very high temperatures, usually around 3000 K, and some of the electrons gain enough kinetic energy to simply overcome the workfunction barrier and leave the Fermi level for the vacuum level. A small externally-applied electric field will then pull these electrons in the desired direction. In field-electron emission, or field-emission (FE) for short, a very high external field (on the order of a few volts per nanometer or higher) is applied to the source, such that the vacuum level is significantly lowered just

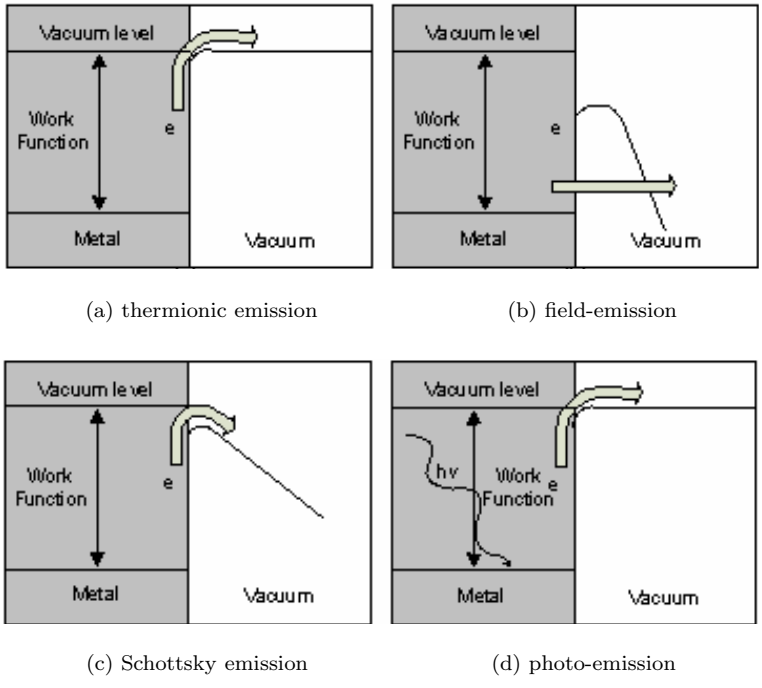

(a) thermionic emission (b) field-emission

(c) Schottsky emission (d) photo-emission

Fig. 2. Various electron emission mechanisms.

outside the surface and only a thin energy barrier remains between the electrons and vacuum. Thus, through the process of quantum-mechanical tunneling, some of the electrons go directly to the vacuum without having to acquire enough energy to overcome the barrier. This phenomenon was modeled by Fowler and Nordheim in 1928[1] and their model is still in widespread use in studying field-electron emitters. A combination of relatively strong external fields (less than those required for field-emission) and high temperatures (less than those required for thermionic emission) can also lead to the so-called Schottky emission. Another emission mechanism, which is widely studied, is photo-electron emission, or photo-emission for short, where photons with energies higher than the workfunction of the electron source illuminate it and transfer enough energy to the electrons to overcome the emission barrier, similar to thermionic emission. Figure 2 provides a schematic representation of these various electron emission mechanisms.

Several parameters determine how an electron emitter will perform in an electron-optical system. Of particular importance are the brightness, energy spread, noise, stability and lifetime. Brightness is the amount of current density that the source can emit into the unit spatial solid angle, and directly affects how "sharp" a beam will be formed. This imposes a limit on resolution in lithography and microscopy by affecting not only the signal to noise ratio in detection, but also the beam spot at the focal plane due to geometrical aberrations. The energy spread of

the emitted electrons affects the beam spot at the focal plane, and therefore the resolution, through chromatic aberrations: the higher the variety of the electron energies in the emitted beam, the harder for the electron-optical system to focus all the electrons to the same spot. Noise, such as Shot noise due to the random emission of electrons in time, can have a significant impact on not only the signal to noise ratio in applications such as microscopy, but also the accuracy of the delivered dose in lithography. Finally, the stability of the emitted current over time and the lifetime of the electron source are also important considerations.

3. Carbon Nanotubes

Carbon nanotubes (CNTs) consist of one or more rolled layers of graphene, which is a sheet of carbon atoms with a thickness of one atom arranged in a hexagonal lattice like a chicken wire. The direction in which the graphene sheet must be wrapped to create a given nanotube is represented by a vector (n, m) called the chiral vector. The integers n and m denote the number of unit vectors along two directions in the honeycomb crystal lattice of graphene. If $m = 0$, the nanotube is called "zigzag". If $n = m$, the nanotube is called "armchair". Otherwise, it is called "chiral" (Fig. 3).

The chemical bonding between the neighboring atoms in CNTs is of sp^2 hybrid type, similar to that of graphene. This bonding structure, which is even stronger than the sp^3 bonds found in diamond, provides the molecules with their unique strength. Thus, CNTs are among the strongest and stiffest materials known, with an elastic modulus in the TPa range. Combined with their low density of 1.3–1.4 g/cm^3, this makes them suitable for very high strength to weight ratio applications. Based on its geometry, namely its chirality and diameter, a CNT can be metallic or semiconducting. With lengths of up to centimeters demonstrated experimentally, CNTs have very high aspect ratios, virtually making them one-dimensional, leading to high transmission and even ballistic transport for electrons. Together with their

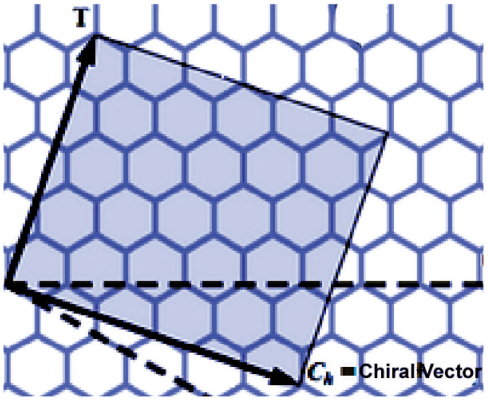

Fig. 3. The hexagonal lattice of graphene and the unit vectors — rolling the graphene up along different directions will lead to nanotubes with various chiralities.

ability to carry current densities of up to 10^9 A/cm^2 (orders of magnitude higher than copper and silver), this makes them very attractive for electronic applications.

CNTs can be fabricated with various methods, most notably arc discharge, laser ablation and chemical vapor deposition. In arc discharge, a high discharge current blows carbon atoms out of a graphitic target (that could also contain catalytic metal) in a chamber. The carbon atoms then deposit in the form of nanotubes on a substrate. CNTs were first discovered by this method.[2] In laser ablation, a pulsed laser vaporizes the graphitic target in a high-temperature reactor in the presence of an inert gas. As the laser ablates the target, nanotubes are formed and carried by gas flow to a cooler surface in the reactor. This method has a yield of about 70%.[3] Chemical vapor deposition (CVD) consists of decomposing hydrocarbons using high temperature and in the presence of catalyst material, and having the extracted carbon form nanotubes emanating from the catalyst island. It is a very common method for device fabrication since it allows one to directly grow CNTs in desired locations (pre-patterned catalyst islands) as opposed to other methods, which require the collection of CNTs after their growth and placing them in desired spots on a substrate. The gases commonly used for CNT growth are: a carrier gas such as hydrogen or argon and carbon containing gases such as ethylene or methane. The reaction temperature is usually in the 700–900°C range. The catalyst material primarily consists of transition metal nanoparticles.

Due to their sharp geometry (high aspect ratio and small tip radius), which leads to significant enhancement of an externally applied electric field, the ability to carry extremely high current densities, mechanical strength and chemical stability, CNTs seem like ideal candidates for electron emission applications. Moreover, their one-dimensionality and the strong presence of quantum effects in them create interesting opportunities for unusual emission characteristics that could be exploited for many novel applications. Good review articles on carbon nanotubes have been published in the past. A good example is one by de Jonge and Bonard.[4]

4. Field-Electron Emission from Individual Nanotubes

In 1928, R. Fowler and L. Nordheim proposed a model for electron emission from metals in an intense electric field. The model assumes that the source has a metallic density of states, the material is at ordinary temperature, and electrons face a one-dimensional potential barrier. This model leads to a current density equation of the form:

$$J = aE^2 \exp\left[-\frac{b}{E}\right], \tag{1}$$

where a and b are constants. Generally for emission from a metallic emitter, (1) is graphically expressed on $\ln[\frac{J}{E^2}]$ versus $\frac{1}{E}$ scales, which would lead to a straight line.

Currently, carbon nanotubes are intensively studied for field-emission. It has widely been assumed that because of their metallic or semi-metallic properties, their

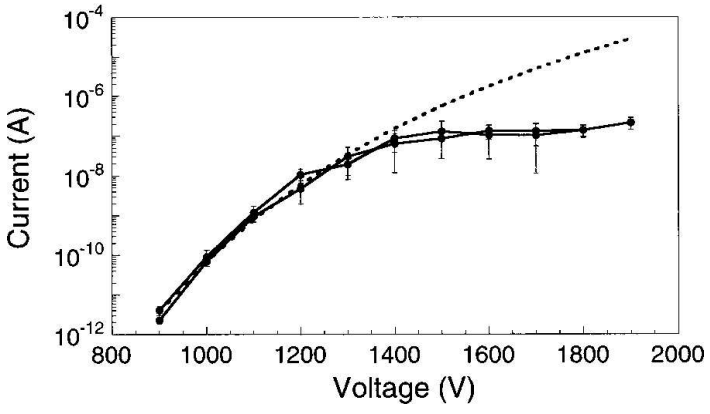

Fig. 4. The current saturation behavior of an individual SWNT — the dashed line is a Fowler–Nordheim equation fit to the low voltage data.[10] Reprinted with permission from K. A. Dean and B. R. Chalamala, *Appl. Phys. Lett.* **76** (2000) 375. Copyright (2000), American Institute of Physics.

field-emission behavior can be explained by the Fowler–Nordheim (FN) model. In this section and Sec. 5, some of the research on field-emission from individual and collections of CNTs is discussed, with a strong emphasis on the degree to which the FN model could be applicable. Although current saturation at high fields in CNTs is a generally accepted behavior, both linear and nonlinear FN curves are presented in the literature.

4.1. *Single-walled carbon nanotubes (SWNTs)*

SWNTs have been investigated by many researchers for their field-emission (FE) properties. Due to the irreproducibility of their growth and thus performance, their practical applications have been minimal at best. However, their excellent properties have enticed researchers to investigate their emission properties in detail.

One of the most noted properties of FE from CNTs is their current saturation behavior at high fields.[5–9] Kenneth *et al.* demonstrated this by setting up a SWNT in a point-to-plane electrode geometry and performing FE experiments in a field-emission microscope (FEM).[10] Figure 4 illustrates their results and shows a reversible current saturation behavior. This behavior would lead to a nonlinear FN plot, and was explained by the authors to be caused by contact resistance, vacuum space charge, and most importantly, adsorbates (H_2O in their experiments). As a result of field and current-induced decrease in the tunneling enhancement of the adsorbate states, adsorbates saturate the current.

In our own experiments on FE properties of SWNTs lying on a dielectric [Fig. 5(a)], a nonlinear FN curve was observed [Fig. 5(b)].[11] We believe this nonlinearity to be partially due to the fact that the FN formulation is for a flat metal surface and cannot be directly applied to a complex three-dimensional structure

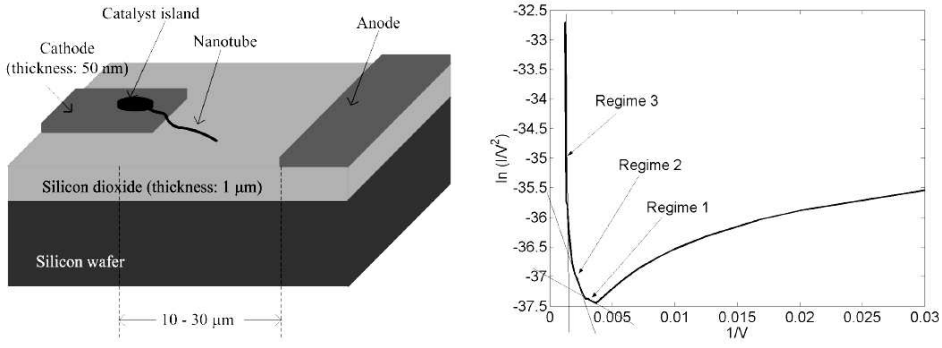

Fig. 5. (a) Schematic of a surface nanotube electron emitter. (b) Emission current versus applied voltage potted on an FN scale.[11] (© 2007 IEEE)

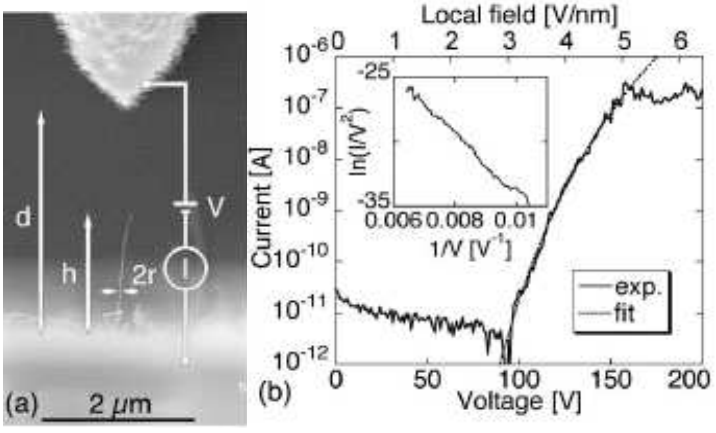

Fig. 6. (a) Scanning electron micrograph of a nanotube of length $h = 1.4$ μm and radius $r = 7.5$ nm with a sharp anode positioned at a distance $d = 2.65$ μm. (b) The corresponding I–V curve with a fit to the FN law in the dotted line. The FN plot is given in the inset.[13] Reprinted figure with permission from J.-M. Bonard, K. A. Dean, B. F. Coll and C. Klinke, *Phys. Rev. Lett.* **89** (2002) 197602. Copyright (2002) by the American Physical Society.

like a CNT on a surface. Also, the density of states at the tip of the CNT is not necessarily metallic and, as shown by Zheng *et al.*, there could exist a nanoscale potential well at the tip that significantly affects the electronic structure.[12]

4.2. *Multi-walled carbon nanotubes (MWNTs)*

Bonard *et al.* investigated the emission from individual MWNTs by isolating them from a MWNT film using a sharp anode [Fig. 6(a)].[13] Similar to SWNTs, MWNTs show a current saturation behavior [Fig. 6(b)].

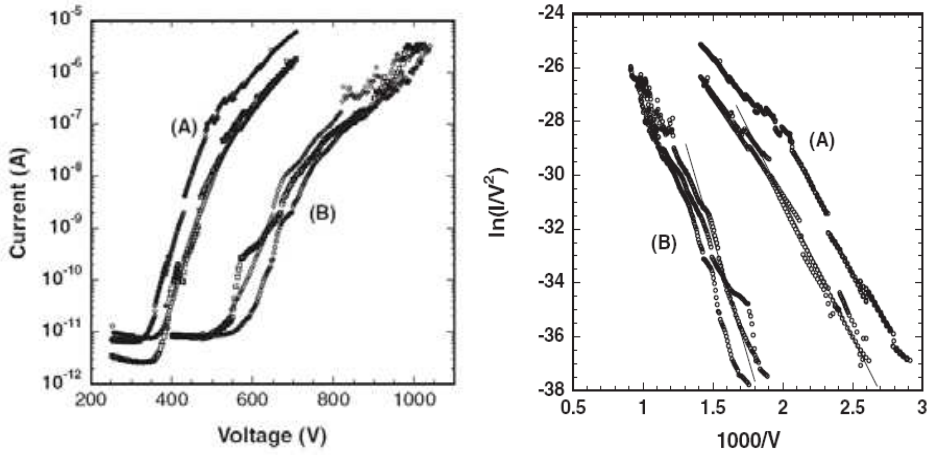

(a) (b)

Fig. 7. (a) *I–V* characteristics of a MWNT with amorphous carbon on tip before (Group B) and after (Group A) the heat treatment. For the heat treatment, the tungsten tip was heated to 700 K during the field emission at 800 V. (b) FN plot of the data with straight line fits in lower voltage regions.[14] Reprinted with permission from H. Tanaka, S. Akita, L. Pan and Y. Nakayama, *Jpn. J. Appl. Phys.* **43** (2004) 864. Copyright (2004), Japanese Journal of Applied Physics.

Tanaka *et al.* investigated FE from a stand-alone MWNT.[14] They deposited amorphous carbon on its tip to create an insulating layer. They performed electron emission experiments and then they removed the insulating layer by using heat treatment. When the insulating layer was removed, the turn on voltage decreased by 200 V, and the increase rate of current with voltage became higher. The *I–V* characteristics of these MWNTs are shown in Fig. 7(a) for before and after heat treatment. A current saturation behavior is apparent, and the corresponding FN plot deviates from a single straight line as shown in Fig. 7(b).

Xu *et al.* performed *in situ* electron emission experiments from an individual MWNT in a transmission electron microscope (TEM). They investigated both the field enhancement factor[15] and the work function.[16] They varied the distance between the MWNT and the anode and measured the field enhancement factor. The measured *I–V* characteristics and FN plots are shown in Fig. 8. Their results show a linear FN behavior and also a non-saturating *I–V* plot.

For calculating the nanotube work function, they resonated a MWNT to its mechanical resonance by applying an alternating electric field and then adding a DC voltage to the alternating voltage. According to the principle of contact potential difference, the DC voltage at which the MWNT stops resonating is the workfunction of the nanotube tip. By being able to calculate an accurate workfunction, they were able to fit a more accurate FN relationship to their experimental results (shown in Fig. 9). The FN plot is again linear and no current saturation behavior is observed.

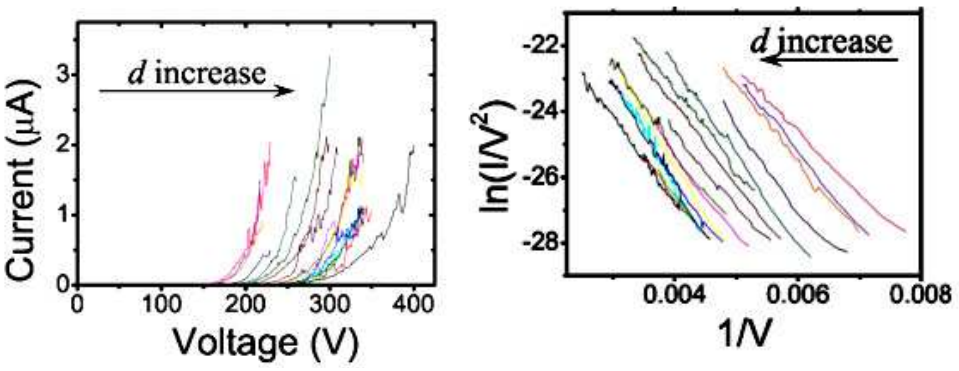

(a) (b)

Fig. 8. (a) *I–V* curves of the field emission for different nanotube–anode distances *d*. (b) The corresponding FN plots.[15] Reprinted with permission from Z. Xu, X. D. Bai and E. G. Wang, *Appl. Phys. Lett.* **88** (2006) 133107. Copyright (2006), American Institute of Physics.

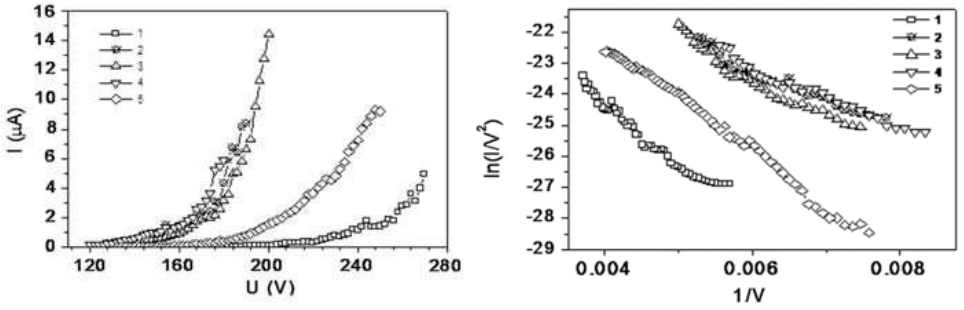

(a) (b)

Fig. 9. (a) *I–V* curves of five different nanotubes. (b) The corresponding FN plots.[16] Reprinted with permission from Z. Xu, X. D. Bai, E. G. Wang and Z. L. Wang, *Appl. Phys. Lett.* **87** (2005) 163106. Copyright (2005), American Institute of Physics.

One of the important performance factors of an electron source is its brightness. de Jonge *et al.* tested this property by using a MWNT as an electron source in a point projection microscope.[17] This setup allowed them to estimate the radius of the source by counting the number of visible fringes made by a sharp edge touching the beam from the side. With a known radius of the source, they calculated the reduced brightness of the MWNT to be an order of magnitude larger than the current state-of-the-art electron sources. They also measured the brightness versus energy spread for the nanotube source (Fig. 10).[18]

In an atypical experiment, Chai and Chow investigated electron emission from the sidewall of a looped MWNT (Fig. 11).[19] Their result did follow the FN model. Interestingly, the FN data gave them a field-enhancement factor of about 400,000, which is much higher than is usually obtained for emission from a nanotube tip. As

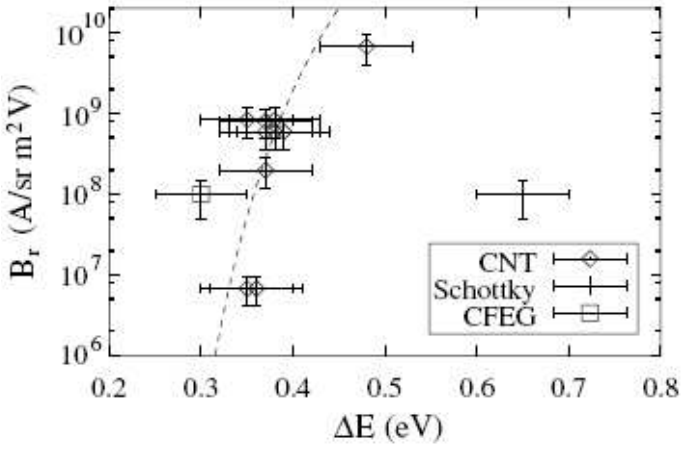

Fig. 10. Brightness (B_r) as a function of energy distribution (ΔE) measured for several CNTs at currents of 10–500 nA and temperatures of 600–700 K. Calculated curve (dashed line). The data of the Schottky emitter and the tungsten cold field emission gun are also included.[18] Reprinted figure with permission from N. de Jonge, M. Allioux, J. T. Oostveen, K. B. K. Teo and W. I. Milne, *Phys. Rev. Lett.* **94** (2005) 186807. Copyright (2005), by the American Physical Society.

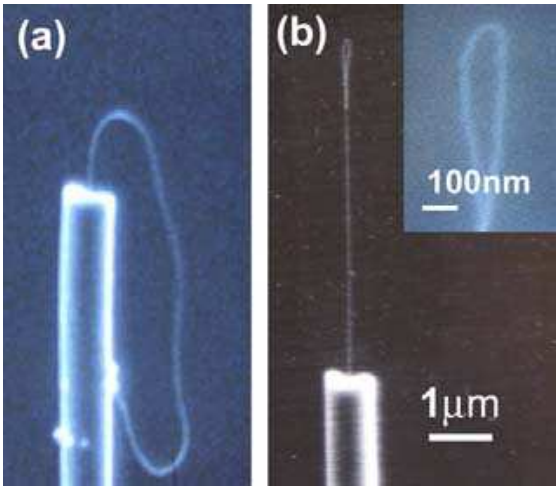

Fig. 11. Nanotube sidewall emitter.[19] Copyright (2007), with permission from Elsevier.

they point out, this result is completely counter-intuitive. Another way of fitting the FN data was the possible reduction in the nanotube work function due to the induced curvature. Their device fabrication process involved bombardment of the nanotubes by Ga ions to create the loop. They also speculate that the defects created by the ions on the sidewall might be at the root of the improved emission properties. Nonetheless, the emission characteristics were stable and reproducible.

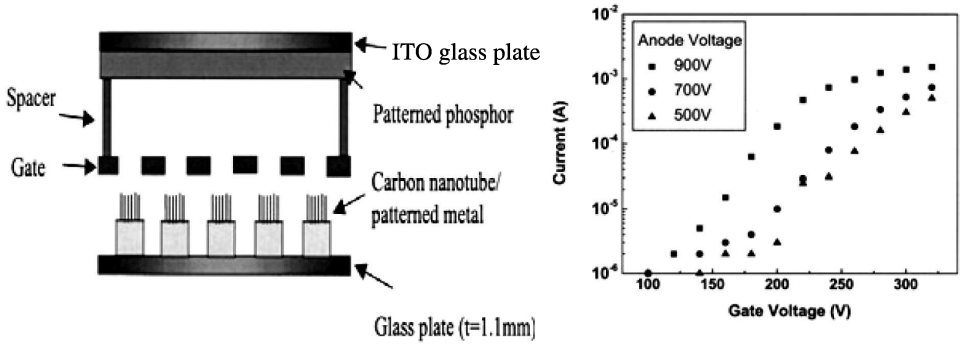

(a) (b)

Fig. 12. (a) Schematic geometry of a triode-type carbon nanotube-based field emission display. (b) Emission current of a triode type CNT-FED for various anode voltages.[20] Reprinted with permission from W. B. Choi *et al.*, *Appl. Phys. Lett.* **78** (2001) 1547. Copyright (2001), American Institute of Physics.

5. Field-Electron Emission from Collections of Nanotubes

5.1. *SWNTs*

Collections of CNTs have more reproducible electron emission characteristics than individual CNTs since recreating exactly the same individual nanotube is difficult, whereas the average behavior of a large ensemble of nanotubes is reproducible. One of the major applications of collections of CNTs is in field-emission displays (FEDs). Various fabrication methods have been exploited in order to obtain the simplest and most reliable FEDs. Choi *et al.* demonstrated a triode type FED using SWNTs [Fig. 12(a)].[20] The I–V characteristics of this triode-type FED are shown in Fig. 11(b) and the current saturation behavior is apparent. Such behavior, as noted before, will lead to a nonlinear FN curve.

Lee *et al.* fabricated an organic flexible array of SWNTs by using self-assembled monolayers.[21] They also observed current saturation behavior [Fig. 13].

Bonard *et al.* also observed such current saturation behavior in their experiments on films of SWNTs (Fig. 14).[6] They attribute this to space charge effects, light emission coupled with field-emission, and the difference in electron distribution between the tube and the tip. Zheng *et al.* have shown that at the tip where emission occurs, the local density of states presents sharp localized states that are close below the Fermi level and are dependant on the tip geometry.[12] The presence of these localized states could explain the current saturation behavior commonly noted in CNTs.

5.2. *MWNTs*

Films of MWNTs produce the most reliable form of FE among the different configurations of CNTs. Collins *et al.* fabricated a film by using MWNTs made by

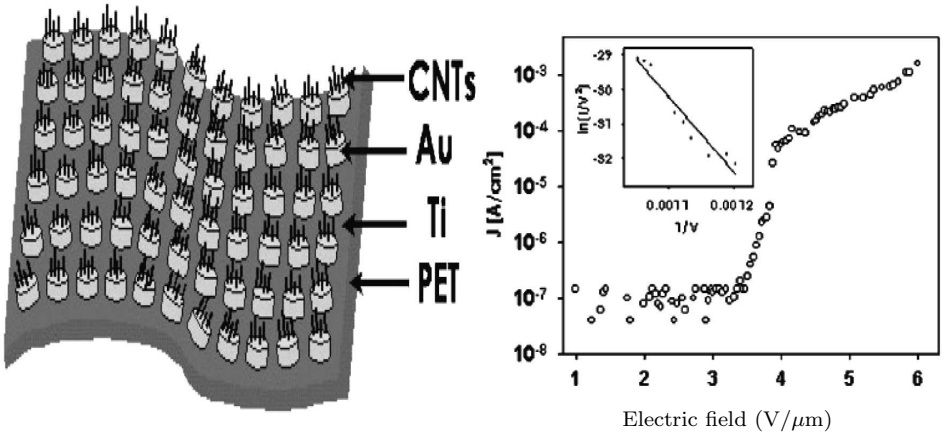

Fig. 13. (a) Schematic diagram of the flexible substrate and aligned carbon nanotubes. (b) Emission current density versus electric field for the emitter. Inset: FN plot.[21] Reprinted with permission from O.-J. Lee and K.-H. Lee, *Appl. Phys. Lett.* **82** (2003) 3770. Copyright (2003), American Institute of Physics.

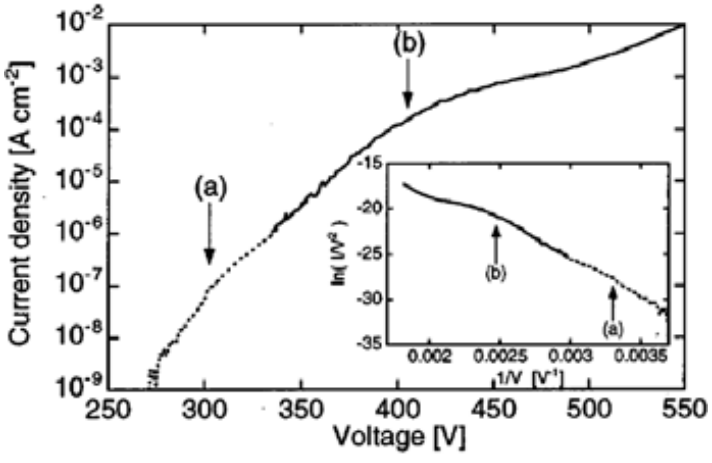

Fig. 14. Single I–V characteristics of a typical SWNT film. Inset: the corresponding FN plot. Arrows (a) and (b) indicate the end of the low current regime and the onset of the saturation, respectively.[6] Reprinted with permission from J.-M. Bonard, J.-P. Salvetat, T. Stockli, W. A. de Heer, L. Forro and A. Chatelain, *Appl. Phys. Lett.* **73** (1998) 918. Copyright (1998), American Institute of Physics.

arc discharge and mixing them with an epoxy.[8] This mixture was then dried by applying pressure. Their electron emission I–V curve is shown in Fig. 15(a) for an onset voltage (V_{ons}) of 100 V, where V_{knee} defines the point where the collected data deviates from low voltage behavior. The result was further analyzed by plotting the FN curve, where the nonlinear behavior is again noted [Fig. 15(b)].

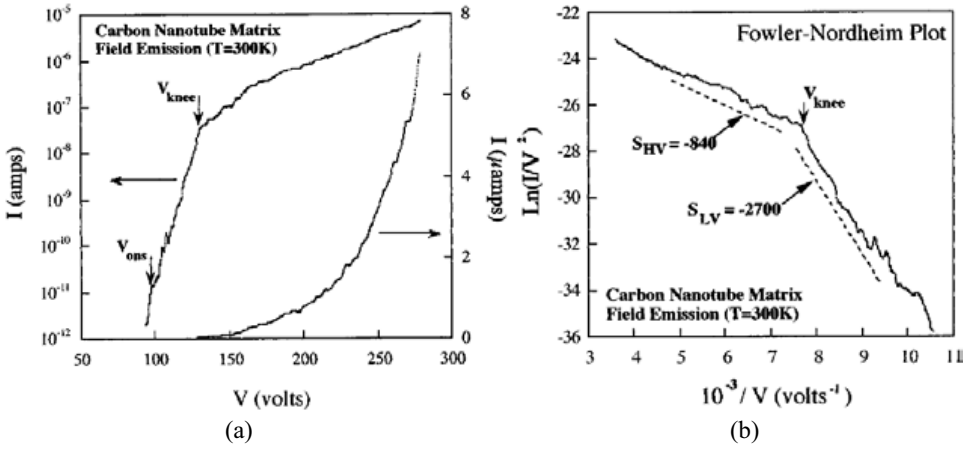

Fig. 15. (a) I–V curve for field-emission from a MWNT matrix sample — it shows both logarithmic and linear current scales. (b) The corresponding FN plot.[8] Reprinted figure with permission from P. G. Collins and A. Zettl, *Phys. Rev. B* **55** (1997) 9391. Copyright (1997), by the American Physical Society.

This non-conformity to a single-straight-line FN behavior was said to be caused by the following reasons:

(i) Space charge surrounding the emission site would reduce the actual electric field at the tip at high current densities.[22]
(ii) Limited carrier concentration in a nonmetallic emitter could add to or exaggerate the space-charge effect.
(iii) Nanotubes might have localized states at the tip that are weakly coupled to the bulk.
(iv) Emission from multiple sources is not taken into consideration when using FN equations.
(v) The non-emitting CNTs could create a large electric field that would create a complex field distribution, not taken into account in the FN model.
(vi) CNTs that are below the epoxy could cause dielectric breakdown at high electric fields, tunnel through, and emit electrons.

This behavior was modeled by Latham and Wilson, who describe a situation where the electronic properties of the insulating layer dominate the I–V characteristics as opposed to the emitter itself.[23]

Films of MWNT are also used for FEDs. Kwo *et al.* tested the characteristics of a FED by using such a film.[24] It was made by a printing process, where the slurry of MWNTs was adhered to the electrode through heat treatment. The FE properties of the films were tested, and the emission I–V plot and the FN plot are shown in Fig. 16.

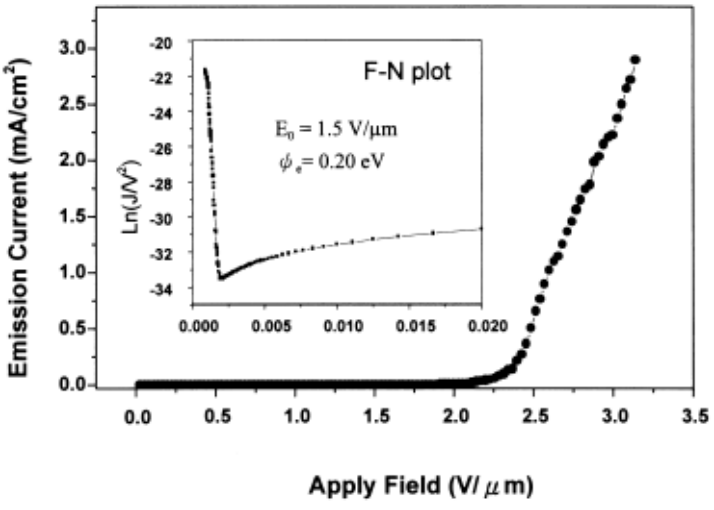

Fig. 16. *I–V* characteristics of CNT clusters synthesized by arc discharge with 150 A arc current and 20 V arc voltage, under 500 mbar (He). The inset shows the corresponding FN plot.[24] Reprinted from J. L. Kwo, M. Yokoyama, W. C. Wang, F. Y. Chuang and I. N. Lin, *Diamond and Related Materials* **9** (2000) 1270. Copyright (2000), with permission from Elsevier.

6. Other Traditional Emission Mechanisms

As discussed in Sec. 2, field-emission is only one of several possible ways of extracting electrons from a source. Other mechanisms include thermionic emission, photo-emission, or a combination of any of those. Traditionally, field-emitters have provided higher-quality electron beams in terms of brightness and energy spread, and perhaps that is one of the reasons why there has been so much work on field-emission from nanotubes, and much less on other emission mechanisms. Nonetheless, we feel that the other mechanisms are also important and in this section shall briefly review some of the related work. In many cases, a combination of thermionic and field-emission was studied.

Chernozatonskii *et al.* investigated the effect of temperature on the FE of thin-film nanotube samples — both single-walled and multi-walled. They observed that in the range of voltages before FE starts, the emission behavior seems to follow the Richardson–Deshman–Schottky law for the temperature range under study (up to 745 K).[25] After FE started, they observed that the FN behavior was adjusted for the effect of temperature (significantly increased).

The effect of direct heating and laser heating on FE of MWNTs was also investigated by Chen *et al.*[26] They reported a factor of almost 50 times increase in field-emission current when the sample was heated from room temperature to 700 K. They also noted a decrease in the turn-on field as a result of an increase in temperature. Koeck *et al.* also reported enhancement of about 30 times in the field-emission current of a CNT film with a temperature change from 380°C to 750°C.[27]

Cox *et al.* experimented with MWNTs grown by CVD at low temperature.[28] They believe that the low-temperature growth condition leads to defective nanotubes with poor thermal conductivity. When electric current was passed through these nanotubes, they observed electron emission from them when the amount of electric power dissipated in the nanotubes was in excess of 100 μW. Their estimate is that the peak thermionic emission happens at a nanotube temperature of around 2900 K.

Another very interesting work on thermionic emission from nanotubes is that of Liu *et al.*[29] They mounted a MWNT yarn in a hairpin configuration, much like a traditional tungsten thermionic emitter. They analyzed the luminescence spectra from the heated yarn to determine the temperature. At anode voltages below the onset of field-emission, they attribute all the emission current to thermionic emission. Their emission curves have the same features as thermal FE from tungsten. By using Richardson's law, they determined the workfunctions of their samples to be in the 4.54–4.64 eV range. The full-width-at-half-maximum of the energy distribution of the emitted electrons was about 0.8 eV at 2024 K.

As discussed before, another mechanism to excite electrons out of a source is photo-emission, where light particles transfer energy to electrons to overcome the workfunction barrier. The electron source in this case would be called a "photocathode". Typically, since the workfunction of nanotubes is in the 4–5.5 eV range, ultra-violet light is necessary to generate photo-electrons. One interesting experiment was done by Wong *et al.*, where they studied photo-emission from a film of MWNTs.[30] They used wavelengths of 266 nm, 355 nm and 532 nm to excite the emission. At low laser energy, with 266 nm (corresponding to a photon energy of 4.66 eV), they observed a one-photon assisted emission process. This was not the case with the other two wavelengths, which corresponded to photon energies significantly less than the nanotube workfunction. Even with 266 nm, the quantum efficiency of the sample was small since, as explained by the authors, a large number of the nanotubes have workfunctions even higher than 4.66 eV. At high laser energies, they observed a notable rise in the emission signal as a function of laser energy for all three wavelengths, indicating a thermally-assisted field-emission process.

7. Novel Electron Emission Mechanisms

So far, we have focused on more traditional methods of electron emission from nanotubes, namely field-electron emission, thermionic emission and photo-electron emission. In this section, we will discuss an experiment where electron emission happens at least partially due to other mechanisms, which could possibly be quite particular to the nanotube structure.

A SWNT device was made where individual nanotubes were lying on a surface, connected to microfabricated electrodes which apply the field.[31] Electron emission experiments were performed inside an SEM. An external electric field, just below

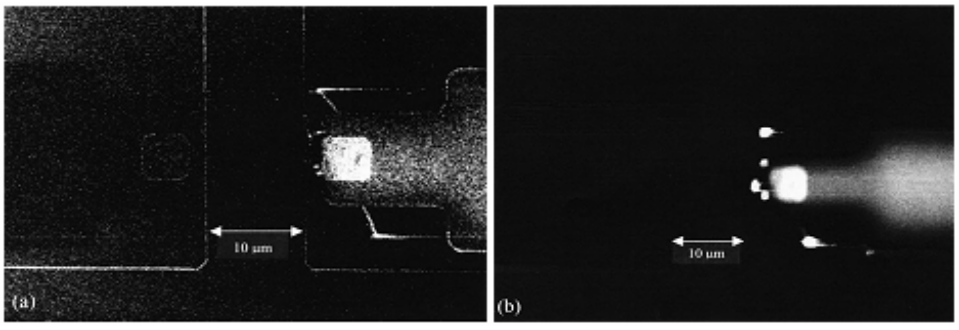

Fig. 17. Bright spots at the nanotube tips as a result of beam-stimulated field-emission. The wide semi-bright area on the right is the cathode electrode and the square is the nanotube growth catalyst island.[32] Reprinted with permission from A. Nojeh, W.-K. Wong, A. W. Baum, R. F. Pease and H. Dai, *Appl. Phys. Lett.* **85** (2004) 112. Copyright (2004), American Institute of Physics.

the threshold value necessary for field-emission, was applied to the device. Since the magnitude of the field was not high enough to drive electron emission, under these circumstances another agent was necessary to trigger the emission process. The primary beam of the SEM was used for this purpose. Thus, every time the primary beam scanned past the tip of the biased nanotubes, the tips emitted for a short period of time, leading to a momentary saturation of the secondary electron detector of the SEM and a bright spot at the nanotube tip on the image. Remarkably, although the nanotube tip is a very small area of a hollow structure and does not provide a bulk for interaction with the primary electrons, the electrons seem to interact very strongly with the tip, and the electron gain (from the primary to the emitted secondaries) was observed to be very high (estimated to be up to about 100). This beam-stimulated field-emission phenomenon was used to obtain a visual map of the emission hot-spots of a carbon nanotube emitter (Fig. 17) to ensure that the nanotubes, and not other areas of the structure such as electrodes or catalyst material, are the active emitting parts of the device.[32]

8. Observation of Emission Sites

One of the major difficulties in experiments and measurements on nanoscale devices arises from the fact that typically the main part of the device, such as a nanotube, is surrounded by larger, microscale, structures such as metal electrodes or catalyst islands that could severely affect the measurement results. In electron emission, this becomes particularly important since a sharp protrusion on the electrodes or catalyst can greatly contribute to the emission current, thus masking the real nanotube emission characteristics. It is therefore extremely important to be able to visualize the emission hot-spots on a device.

Fujieda *et al.* performed electron emission from a MWNT inside a transmission electron microscope, were they were able to see a bright spot on the nanotube tip

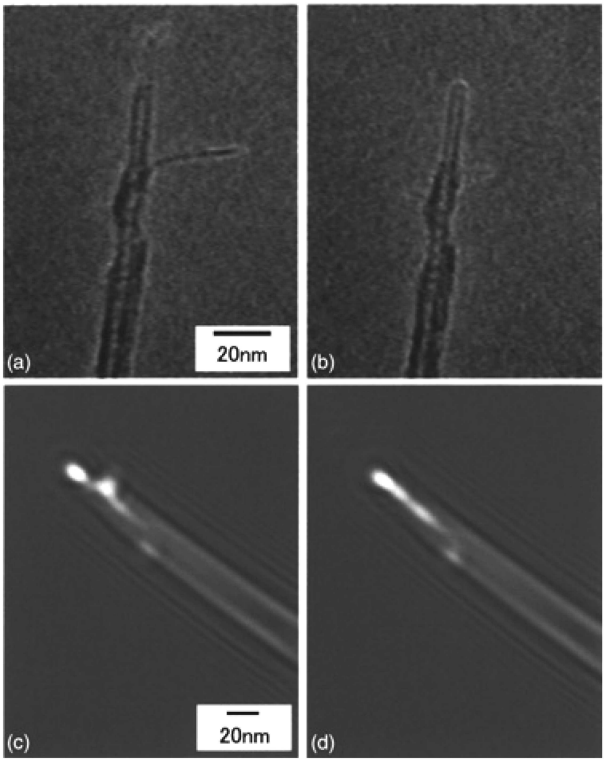

Fig. 18. Bright emission spot at a nanotube tip emitting electrons, imaged in a transmission electron microscope, and structural damage to the nanotube tip.[33] Reprinted with permission from T. Fujieda, K. Hidaka, M. Hayashibara, T. Kamino, H. Matsumoto, Y. Ose, H. Abe, T. Shimizu and H. Tokumoto, *Appl. Phys. Lett.* **85** (2004) 5739. Copyright (2004), American Institute of Physics.

(Fig. 18). They were also able to observe the correlation between the structural damage at the emitting tip and large fluctuations happening at high emission currents.[33] They conjecture that the mechanism behind the formation of this bright spot is the interference between the primary electrons passing through the nanotube deflected due to field-emission and those passing outside of the nanotube unaffected by field-emission.

Field-emission electron microscopy and photo-emission electron microscopy are well-established techniques to visualize electron emission from a surface. Gupta *et al.* used these techniques to look at the emission sites of both SWNT and MWNT matt samples.[34] By visualizing the emission hot-spots, they observed that although the surface contained more than $10^8/\text{cm}^2$ nanotubes, the emission site density was in the order of $10^4/\text{cm}^2$, making individual emission sites easily visible. By measuring the emission intensity from these sites, they studied the temporal stability and temperature dependence of emission, as well as the role of adsorbates in emission properties. By using a substrate heater, they studied the emission properties

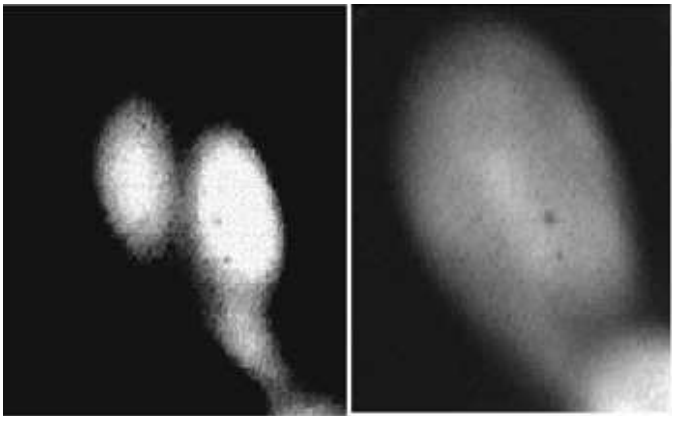

(a) (b)

Fig. 19. Electron emission patterns from a SWNT in a field-emission microscope.[35] Reprinted with permission from K. A. Dean and B. R. Chalamala, *J. Appl. Phys.* **85** (1999) 3832. Copyright (1999), American Institute of Physics.

of the samples up to 1000°C. They obtained up to a three-fold increase in the integrated brightness by this temperature change, which could be related to both direct thermally-assisted emission, and the self-cleaning of the emission sites from chemisorbed molecules, induced by high temperature and field.

Dean and Chalamala performed field-emission microscopy of samples containing SWNTs protruding from the surface for lengths of several microns.[35] They observed the emission patterns corresponding to individual nanotubes [Fig. 19(a)]. The lobed patterns were essentially identical to those obtained as a result of adsorbate atoms and molecules on metallic field-emitters. By heating the sample to temperatures of up to 900 K, adsorbates were removed and the lobed patterns disappeared, revealing the much dimmer emission patterns resulting from the nanotube itself [Fig. 19(b)]. The emission current also had a significant drop. They argue that the obtained images under these conditions do not correspond to individual atoms, but rather depict the surface electronic structure of the localized cap states of the nanotube.

Similar experiments were performed by Hata *et al.* on MWNTs.[36] Again, heat treatment was used to remove the adsorbates and reveal the emission patterns resulting from the nanotube tip. They observed streaks between the bright spots corresponding to adjacent emission sites on the nanotube tip, which they explained in terms of Young's interference fringes. Similar results were obtained by Tanaka *et al.*,[37] which they argued could be explained in terms of both interference and a standing wave along the circumference of the nanotube.

In addition to field-emission microscopy, Kuzumaki *et al.* also performed field ion microscopy of nanotube samples.[38] Thus, they were able to image both the electric field concentration sites and the surface workfunction. From their results, it appears that the pentagonal carbon rings at the tip are not highly-emitting areas.

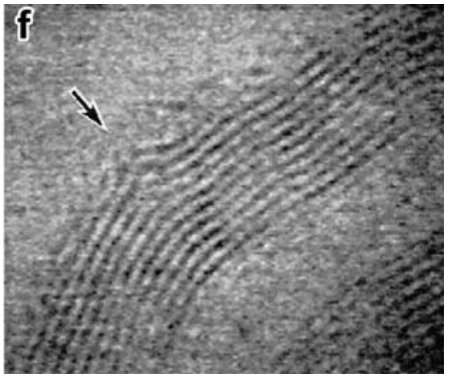

Fig. 20. Deformed nanotube tip as a result of electron emission, seen in a transmission electron microscope.[38] Reprinted from T. Kuzumaki, Y. Horiike, T. Kizuka, T. Kona, C. Oshima and Y. Mitsuda, *Diamond and Related Materials* **13** (2004) 1907. Copyright (2004), with permission from Elsevier.

Thus, they believe that the patterns observed in field-emission microscopy do not correspond directly to emission sites, but are rather the result of the interference of electrons being emitted from various sites as seen in field ion microscopy. They also performed emission experiments while looking at the nanotube tip inside a high-resolution transmission electron microscope, and observed that the nanotube tip becomes deformed and a protrusion is created, possibly by some of the atoms reconfiguring themselves from sp^2 to sp^3 bonding (Fig. 20). Bonard and colleagues also reported field-emission microscopy images very similar to the ones mentioned above,[39] and concluded that the electrons were emitted from localized states at the tip, and not delocalized electrons such as in metals.

9. Modeling and Simulating Electron Emission from Carbon Nanotubes

As for any nanoscale physical modeling and simulation problem, the theoretical study of electron emission from carbon nanotubes presents major difficulties. On one hand, for an accurate theoretical analysis, the system cannot be considered a continuous bulk and treated classically with continuum models and the exact atomistic nature of the structure must be taken into account. On the other hand, typically in a nanotube device, there is a large enough number of atoms that solving the many-body quantum mechanical problem for the entire system is nearly impossible even with the most powerful computers of today. Thus, modeling such systems necessitates being able to identify which aspects of a given problem need to be treated using atomistic simulations and what parts can be analyzed with more approximate, classical representations. Usually, a hybrid approach can be used to keep the problem manageable, while still capturing the essence of the nanoscale physics involved. One such hybrid method has been discussed by Han.[40]

Currently, to the best of the authors' knowledge, a universal theory explaining all aspects of electron emission from carbon nanotubes does not exist. As seen in some of the previous sections, even in the experimental world there is still a debate in the research community on some of the fundamentals of this process, e.g. whether or not a nanotube emitter follows a traditional Fowler–Nordheim behavior. In this section we will review some of the theoretical works on electron emission from nanotubes to shed further light on the topic.

Zhou and Kawazoe performed first-principles calculations within the framework of the linear combination of atomic orbitals for the molecular orbital (LCAO-MO) cluster model on a (5, 5) nanotube containing 18 unit cells (approximately 3.5 nm in length), capped at both ends.[41] Although this nanotube is theoretically metallic, their results showed that the electron emission from the SWNT is not a continuum as in metals, but is rather strongly-dependent on the precise nature of the orbitals at the tip and the link between the tip and body. They also concluded that the emission characteristics could not be described by the FN model, and the experimental results showing such behavior are due to bundle effects, and not directly due to individual nanotubes.

Kim *et al.* used the density functional theory to study capped (5, 5) and (9, 0) nanotubes under electric fields at the level required for field-emission.[42] For the (5, 5) nanotube, although metallic in theory, they found that the effective work-function decreased linearly with the increasing electric field, as opposed to the quadratic dependence typical in metals.

Zhou *et al.* studied field-emission from an open-ended (6, 6) nanotube, also metallic.[43] They used first-principles calculations with LCAO-MO. They found that besides the first row of carbon atoms directly "in touch" with the vacuum, their first neighbors also contributed to the number of emitted electrons significantly.

Typically when performing first-principles calculations on nanotubes, due to the computationally-expensive nature of the work, a short section of a nanotube is used, which cannot reproduce a realistic level of external field enhancement. Thus, it is customary to use a value for the applied field that already includes the field enhancement effect. A different approach was adopted by Luo *et al.*, where they added extra negative charge to the short nanotube to generate the strong electric field.[44] They used the density functional theory to study the potential barrier near the tip. They observed higher transmission and better emission properties for capped nanotubes than open-ended ones (contrary to the observation made by Zhou and colleagues[43]).

Models that take the atomic nature of the nanotube into consideration and use first-principles calculations to study the electronic structure are quite limited in the size of the nanotubes they can handle. As such, in order to study nanotube emitters in the context of real applications, typically one has to resort to semi-classical, continuum models. An example of such a model is the work by von Allmen *et al.*, where they approximated the nanotube with a conductive cylinder to study the field enhancement and emission properties of arrays of nanotubes for application

in field-emission displays.[45] The transmission coefficient, however, was found by solving the one-dimensional Schrödinger equation. They found that there was an optimal nanotube separation/height ratio to achieve maximum current density from the array.

Shimoyama *et al.* also studied arrays of nanotubes by assuming that the nanotubes were continuous, conductive materials with hemispherical caps.[46] The dimensions of the nanotubes they studied correspond to MWNTs. They found that the field strength at the nanotube tip decreased with the increasing nanotube diameter and tip radius of curvature. They also observed that the field strength was significantly reduced when the nanotube density in the array was more than $10^9/\text{cm}^2$ (corresponding to inter-nanotube distances of less than about 300 nm). For nanotube densities less than $10^8/\text{cm}^2$ (inter-nanotube distance of more than 1 micrometer), they found that the field strength was independent of density.

Another very interesting work was done by Zheng *et al.* who studied FE from a micrometer-long (5, 5) SWNT.[12] In order to overcome the challenge of dealing with large numbers of atoms while performing quantum-mechanical calculations, they adopted a hybrid method where a section of the nanotube away from the tip was treated using molecular mechanics. In this way they were able to simulate a realistic experimental situation and field-enhancement was a natural outcome of the simulation (rather than incorporated manually). They observed that most of the field dropped over a region within about 5 nm of the tip, creating a steep potential well in that region. They obtained field-enhancement factors in the 300–1200 range, confirming the previous belief. In contrast to the results of Changwook *et al.*,[42] they found that the emission barrier height was a nonlinear function of the applied field.

Lan *et al.* took the study of nanotube emitters one step further by calculating electron trajectories from nanotube arrays in a display device and investigating the effect of the emitter bias conditions on the display resolution.[47]

As discussed in Sec. 7 in one experiment, the nanotube was biased just below the field-emission threshold and emission was triggered by shining another electron beam on the tip. Typically, when an electron beam hits a bulk material it undergoes multiple scatterings and generates secondary electrons in the process. This can be modeled using a Monte Carlo approach, for instance. However, due to the small interaction volume of the beam with the nanotube tip (in the order of a cubic nanometer of a hollow structure), such models cannot explain the large number of emitted electrons in that experiment. In Ref. 48, the authors created a model to explain this so-called electron-stimulated field-emission effect, where we performed first-principled calculations to study the behavior of the electronic orbitals at the nanotube tip in the presence of an external electron (representing a primary electron from the beam). We observed that one extra electron could shift the nanotube energy levels upward by as much as about 1 eV, thus significantly increasing the tunneling probability and transmission coefficient, leading to high induced field-emission.

A model for calculating both field and thermionic emission currents, taking into account the band structure of the nanotube and using a triangular-shaped potential barrier at the tip, was presented by Tang *et al.*[49] They investigated the competition between those two emission mechanisms and also studied the energy distribution of the emitted electrons.

10. Final Thoughts

In this article, we reviewed some of the important aspects of electron emission from carbon nanotubes, from both experimental and theoretical points of view. Obviously it was impossible to cover all the interesting works that have been done in this area in this brief review. We saw that although many valuable attempts have been made in both directions, there are still disagreements between various experimental results on important issues such as whether or not field-emission from nanotubes follows the traditional Fowler–Nordheim behavior. Also, we are far from having a universal theoretical model describing all the aspects of electron emission from nanotubes. Nonetheless, nanotubes are starting to find their way into real applications. Good examples include the work of Yabushita *et al.*, where they report a compact field-emission SEM with a MWNT bundle cathode,[50] and that of Getty *et al.*, where they report a field-emission electron gun based on a nanotube film for use in a miniaturized reflectron time-of-flight mass spectrometer.[51]

Although the overwhelming majority of the works have focused on field-emission, more recently there has been an increased attention towards thermionic emission as well. Also, other emission mechanisms such as electron-stimulated field-emission have been observed in nanotubes, seemingly due to their particular nanoscale structure. We believe that more peculiar and exotic emission phenomena, with strong signatures from the quantum mechanical nature of nanotubes, could be possible since nanotube structures are so drastically different from traditional bulk metal emitters that we have been used to for a long time. As the quest for better nanotube-based electron emitters and their transfer to the world of real applications continues, in addition to the systematic study of field- and thermionic emission, it seems to be important to look for such novel mechanisms and phenomena that might lead to improved characteristics in emitters, as well as open up possibilities for new applications.

References

1. R. H. F. L. Nordheim, Containing papers of a mathematical and physical character, in *Proc. Royal Society of London, Series A*, Vol. 119 (1928), p. 173.
2. S. Iijuma, *Nature* **354** (1991) 56.
3. N. G. Chopra, L. X. Benedict, V. H. Crespi, M. L. Cohen, S. G. Louie and A. Zettl, *Nature* **377** (1995) 135.
4. N. de Jonge and J.-M. Bonard, Philosophical transactions of the royal society A, *Math. Phys. Eng. Sci.* **362** (2004) 2239.
5. P. G. Collins and A. Zettl, *Appl. Phys. Lett.* **69** (1996) 1969.

6. J.-M. Bonard, J.-P. Salvetat, T. Stockli, W. A. de Heer, L. Forro and A. Chatelain, *Appl. Phys. Lett.* **73** (1998) 918.
7. X. Xu and G. R. Brandes, *Appl. Phys. Lett.* **74** (1999) 2549.
8. P. G. Collins and A. Zettl, *Phys. Rev. B* **55** (1997) 9391.
9. J.-M. Bonard, T. Stčkli, F. Maier, W. A. de Heer, A. Châtelain, J.-P. Salvetat and L. Forró, *Phys. Rev. Lett.* **81** (1998) 1441.
10. K. A. Dean and B. R. Chalamala, *Appl. Phys. Lett.* **76** (2000).
11. A. Nojeh and R. F. W. Pease, in *Electrical and Computer Engineering, Canadian Conference*, 2007, p. 1294.
12. X. Zheng, G. Chen, Z. Li, S. Deng and N. Xu, *Phys. Rev. Lett.* **92** (2004) 106803.
13. J.-M. Bonard, K. A. Dean, B. F. Coll and C. Klinke, *Phys. Rev. Lett.* **89** (2002) 197602.
14. H. Tanaka, S. Akita, L. Pan and Y. Nakayama, *Jpn. J. Appl. Phys.* **43** (2004) 864.
15. Z. Xu, X. D. Bai and E. G. Wang, *Appl. Phys. Lett.* **88** (2006) 133107.
16. Z. Xu, X. D. Bai, E. G. Wang and Z. L. Wang, *Appl. Phys. Lett.* **87** (2005) 163106.
17. N. de Jonge, Y. Lamy, K. Schoots and T. H. Oosterkamp, *Nature* **420** (2002) 393.
18. N. de Jonge, M. Allioux, J. T. Oostveen, K. B. K. Teo and W. I. Milne, *Phys. Rev. Lett.* **94** (2005) 186807.
19. G. Chai and L. Chow, *Carbon* **45** (2007) 281.
20. W. B. Choi *et al.*, *Appl. Phys. Lett.* **78** (2001) 1547.
21. O.-J. Lee and K.-H. Lee, *Appl. Phys. Lett.* **82** (2003) 3770.
22. J. P. Barbour, W. W. Dolan, J. K. Trolan, E. E. Martin and W. P. Dyke, *Phys. Rev.* **92** (1953) 45.
23. R. V. La and D. A. Wilson, *J. Appl. Phys. D* **16** (1983) 455.
24. J. L. Kwo, M. Yokoyama, W. C. Wang, F. Y. Chuang and I. N. Lin, *Diam. Relat. Mater.* **9** (2000) 1270.
25. L. A. Chernozatonskii, Z. Y. Kosakovskaya, Y. V. Gulyaev, N. I. Sinitsyn, G. V. Torgashov and Y. F. Zakharchenko, in *The Eighth International Vacuum Microelectronics Conference* (AVS, Portland, Oregon USA, 1996), p. 2080.
26. Y.-C. Chen, H.-F. Cheng, Y.-S. Hsieh and Y.-M. Tsau, *J. Appl. Phys.* **94** (2003) 7739.
27. F. A. M. Koeck, Y. Wang and R. J. Nemanich, in *Space Tech. & Applic. Int. Forum-Staif* (AIP, Albuquerque, New Mexico, USA, 2006), p. 607.
28. D. C. Cox, R. D. Forrest, P. R. Smith and S. R. P. Silva, *Appl. Phys. Lett.* **85** (2004) 2065.
29. P. Liu, Y. Wei, K. Jiang, Q. Sun, X. Zhang, S. Fan, S. Zhang, C. Ning and J. Deng, *Phys. Rev. B* **73** (2006) 235412.
30. W. Teh-Hwa, M. C. Gupta and C. Hernandez-Garcia, *Nanotechnology* **18** (2007) 4.
31. A. Nojeh, W. K. Wong, E. Yieh, R. F. Pease and H. Dai, *J. Vac. Sci. Technol. B* **22** (2004) 3124.
32. A. Nojeh, W.-K. Wong, A. W. Baum, R. F. Pease and H. Dai, *Appl. Phys. Lett.* **85** (2004) 112.
33. T. Fujieda, K. Hidaka, M. Hayashibara, T. Kamino, H. Matsumoto, Y. Ose, H. Abe, T. Shimizu and H. Tokumoto, *Appl. Phys. Lett.* **85** (2004) 5739.
34. S. Gupta, Y. Y. Wang, J. M. Garguilo and R. J. Nemanich, *Appl. Phys. Lett.* **86** (2005) 063109.
35. K. A. Dean and B. R. Chalamala, *J. Appl. Phys.* **85** (1999) 3832.
36. K. Hata, A. Takakura, K. Miura, A. Ohshita and Y. Saito, *J. Vac. Sci. Technol. B* **22** (2004) 1312.
37. H. Tanaka, S. Akita, L. Pan and Y. Nakayama, *Time(s)* **450** (2004) 500.

38. T. Kuzumaki, Y. Horiike, T. Kizuka, T. Kona, C. Oshima and Y. Mitsuda, *Diam. Relat. Mater.* **13** (2004) 1907.
39. J. M. Bonard, J. P. Salvetat, T. Stöckli, L. Forró and A. Châtelain, *Appl. Phys. A* **69** (1999) 245.
40. S. Han, Seoul National University, 2000.
41. G. Zhou and Y. Kawazoe, *Phys. Rev. B* **65** (2002) 155422.
42. C. Kim, B. Kim, S. M. Lee, C. Jo and Y. H. Lee, *Phys. Rev. B* **65** (2002) 165418.
43. G. Zhou, W. Duan and B. Gu, *Phys. Rev. Lett.* **87** (2001) 095504.
44. J. Luo, L. M. Peng, Z. Q. Xue and J. L. Wu, *Phys. Rev. B* **66** (2002) 155407.
45. P. von Allmen, L. R. C. Fonseca and R. Ramprasad, *Phys. Status Solidi B* **226** (2001) 107.
46. H. Shimoyama, H. Murata and T. Ohye, *Proc. SPIE* **4510** (2001) 163.
47. Y.-C. Lan, C.-T. Lee, Y. Hu, S.-H. Chen, C.-C. Lee, B.-Y. Tsui and T.-L. Lin, *J. Vac. Sci. Technol. B* **22** (2004) 1244.
48. A. Nojeh, B. Shan, K. Cho and R. F. W. Pease, *Phys. Rev. Lett.* **96** (2006) 56802.
49. H. Tang, S. D. Liang, S. Z. Deng and N. S. Xu, *J. Phys. D* **39** (2006) 5280.
50. R. Yabushita, K. Hata, H. Sato and Y. Saito, *J. Vac. Sci. Technol. B* **25** (2007) 640.
51. S. A. Getty, T. T. King, R. A. Bis, H. H. Jones, F. Herrero, B. A. Lynch, P. Roman and P. Mahaffy, in *Micro (MEMS) and Nanotechnologies for Defense and Security* (SPIE, Orlando, FL, USA, 2007), p. 655618.